HEP'97 #295
Submitted to Pa 7, 8, 11
Pl 15

DELPHI 97-113 CONF 95
20 July, 1997

Measurement of Trilinear Gauge Couplings in e^+e^- Collisions at 161 GeV and 172 GeV

Preliminary

DELPHI Collaboration

T.J.V. Bowcock[1], **C. DeClercq**[2], **G. Fanourakis**[3], **D. Fassouliotis**[4], **V. Kostioukhine**[5], **J. Libby**[6], **C. Matteuzzi**[7], **M. McCubbin**[1], **U. Parzefall**[1], **C. Petridou**[4], **H.T. Phillips**[8], **D. Sampsonidis**[3], **R.L. Sekulin**[8], **F. Terranova**[7], **S. Tzamarias**[3], **A. Van Lysebetten**[2], **O. Yushchenko**[5]

Abstract

Preliminary results are given on trilinear gauge boson couplings from data taken by DELPHI at 161 GeV and 172 GeV. Values for WWV couplings ($V = Z, \gamma$) are determined from a study of the reactions $e^+e^- \to W^+W^-$ and $e^+e^- \to We\nu$, using differential distributions from the WW final state in which one W decays hadronically and the other leptonically and total cross-section data from other channels. Limits are also derived on neutral $ZV\gamma$ couplings from an analysis of the reaction $e^+e^- \to \gamma + \textit{invisible particles}$.

Paper submitted to the HEP'97 Conference
Jerusalem, August 19-26

[1]Department of Physics, University of Liverpool, P.O. Box 147, Liverpool L69 3BX, UK
[2]IIHE-Institut Universitaire des Hautes Energies, Pleinlaan 2, B-1050 Brussels, Belgium
[3]Institute of Nuclear Physics, N.C.S.R. Demokritos, P.O. Box 60228, GR-15310 Athens, Greece
[4]Dipartimento di Fisica, Università di Trieste and INFN, Via A. Valerio 2, I-34127 Trieste, Italy
[5]Inst. for High Energy Physics, Serpukhov P.O. Box 35, Protvino, (Moscow Region), Russian Federation
[6]Department of Physics, University of Oxford, Keble Road, Oxford OX1 3RH, UK
[7]Dipartimento di Fisica, Università di Milano and INFN, Via Celoria 16, I-20133 Milan, Italy
[8]Rutherford Appleton Laboratory, Chilton, Didcot OX11 OQX, UK

1 Introduction

One of the most important consequences of the $SU(2) \times U(1)$ symmetry of the Standard Model is the existence of non-Abelian self-couplings of the gauge bosons γ, W and Z^0. Using data taken in the DELPHI detector at LEP in 1996 at centre-of-mass energies 161 and 172 GeV, we have used events from the reactions $e^+e^- \to W^+W^-$ and $e^+e^- \to We\nu$ to study WWV couplings, where $V \equiv Z, \gamma$ and from the reaction $e^+e^- \to \gamma$ + *invisible particles* to study couplings at the $ZV\gamma$ vertex.

The WWV coupling arises in WW production through the diagrams involving s-channel exchange of Z^0 and γ. The Standard Model predicts a charge coupling, described by a parameter g_1^V in an effective WWV Lagrangian $\mathcal{L}_{WWV}$, and a dipole coupling κ_V, with $g_1^V = \kappa_V = 1$ [1]. In a general Lorentz-invariant description of the WWV interaction, other couplings, both CP-conserving and CP-violating, are possible, but their contributions are predicted to be zero in the Standard Model. In searching for deviations from the Standard Model which could signify the presence of new physics, we consider contributions from CP-conserving, gauge-invariant operators of lowest dimension (≤ 6), taking only those which have not been excluded by previous measurements. This leads to three possible contributions, $\alpha_{W\phi}$, $\alpha_{B\phi}$ and α_W, which are related to the charge and dipole couplings defined above and to the quadrupole couplings λ_V in $\mathcal{L}_{WWV}$ by: $\Delta g_1^Z = \frac{\alpha_{W\phi}}{c_w^2}$, $\Delta\kappa_\gamma = \alpha_{W\phi} + \alpha_{B\phi}$, $\Delta\kappa_Z = \alpha_{W\phi} - \frac{s_w^2}{c_w^2}\alpha_{B\phi}$ and $\lambda_\gamma = \lambda_Z = \alpha_W$, where s_w and c_w are the sine and cosine of the Weinberg angle and Δg_1^Z, $\Delta\kappa_\gamma$ and $\Delta\kappa_Z$ represent deviations from Standard Model values [1].

The process $e^+e^- \to \gamma$ + *invisible particles* is described within the Standard Model by the radiative production of neutrino-antineutrino pairs, $e^+e^- \to \nu\bar{\nu}\gamma$. A W fusion diagram, containing a $WW\gamma$ coupling, also contributes to $\nu\bar{\nu}\gamma$ production, but its amplitude is very small at LEP2 energies, and its relative contribution is negligible. Possible new physics contributions to single photon production could come from a new generation of neutrinos, from the radiative production of any other neutral weakly interacting particle, or from the s-channel exchange of γ or Z, leading to $Z\gamma$ production via a triple vector boson coupling. In this paper we examine this latter possibility. The $ZV\gamma$ vertex has been described by Baur and Berger [2] in terms of a vertex function involving four independent terms $h_{1..4}^V$; in the Standard Model all of these are zero at tree level. The parameters are normally described by a form factor representation, $h_i^V(s) = h_{i0}^V/(1 + s/\Lambda^2)^n$, with an energy Λ representing the scale at which a novel interaction would become manifest, and with a sufficiently large power n to ensure unitarity conservation at high energy. Conventionally, $n = 3$ is used for $h_{1,3}^V$ and $n = 4$ for $h_{2,4}^V$. The terms in h_1 and h_2 are CP-violating, and those in h_3 and h_4 CP-conserving. However, the minimum dimensionality of contributing gauge-invariant operators to $\mathcal{L}_{ZV\gamma}$ is 8 [3], so the observation of deviations from Standard Model predictions is *a priori* less likely in this channel than in those involving WWV couplings.

Results on WWV couplings have previously been reported in $\bar{p}p$ experiments [4, 5, 6], and in first reports of results at LEP2 [7, 8]. Limits on $ZV\gamma$ couplings have been determined in $\bar{p}p$ experiments [4, 6, 9] and from LEP data taken at the Z^0 [10] and at 130-136 GeV [11].

In the next section of this paper we describe the selection of events from the data and the simulation of the various channels involved in the analysis. Results on the trilin-

ear gauge coupling parameters describing the WWV and $ZV\gamma$ vertices are reported in sections 3 and 4 respectively and a summary is given in section 5.

2 Event selection and simulation

In 1996, DELPHI recorded integrated luminosities of 10.0 _and 9.98 _at centre-of-mass energies of 161 and 172 GeV, respectively. Data from several final state topologies were used in the analyses described in this paper.

2.1 Selection of events for the study of WWV couplings

In the determination of WWV couplings, events were selected in the following final state topologies: the "semileptonic" topology ($jj\ell\nu$) required the observation of two hadronic jets and an isolated lepton, the "two jets and invisible lepton" topology (jjX) required the presence of two jets and missing energy, the "single visible lepton" topology (ℓX) required a muon or electron coming from the interaction point, but no other track in the detector, the "fully hadronic" topology ($jjjj$) required the presence of four hadronic jets, and the "2 visible leptons" topology ($\ell\nu\ell\nu$) required two identified leptons coming from the interaction point. The criteria imposed in the assignment of events to each of these topologies, and the estimated selection efficiencies and composition of the selected samples are given below. Details of the DELPHI detector may be found in [12], and the criteria defining track selection and lepton identification have been given in [7].

$jj\ell\nu$:
Events in which one W decays into $\ell\nu$ and the other into quarks are characterized by two hadronic jets, one isolated lepton (coming either from W decay or from the cascade decay W $\rightarrow\tau...\rightarrow\ell...$) or a low multiplicity jet due to τ decay, and missing momentum resulting from the neutrino. The major background comes from $q\bar{q}(\gamma)$ production and from four-fermion final states containing two quarks and two leptons of the same flavour.

The criteria used to define the 161 GeV sample have been given in [7] and resulted in selection of 12 $jj\ell\nu$ events.

In the analysis of data at 172 GeV, it was required that events contain at least 6 charged particles with total energy of at least $0.15\,E_{cms}$. Events with a detected photon unassociated with any charged track and with energy > 20 GeV were rejected. In the case of WW decays into $q\bar{q}\mu\nu$ and $q\bar{q}e\nu$ the candidate lepton was required to be the most energetic charged track in the event, while τ candidates were selected by looking for an isolated e or μ or a jet of multiplicity ≤ 5 with one charged track and total momentum > 10 GeV/c.

Muon candidates were selected using information from the muon chambers and from the hadron calorimeter. Tracks were required to have momentum > 5 GeV/c, and the isolation angle between the candidate muon and the nearest particle with momentum > 1 GeV/c was required to exceed a value set between 8° and 20°, depending on the quality of the muon identification.

Electron identification was performed by looking for charged tracks with energy deposits in the electromagnetic calorimeters matching the track momentum within 20%, or exceeding 20 GeV. The momentum of the electron was required to be > 5 GeV/c and the

component of the missing momentum transverse to the beam axis, p^t_{miss}, was required to exceed 10 GeV/c. The isolation angle between the candidate electron and the nearest particle with momentum above 1 GeV/c was required to exceed a value between 5° and 20°, depending on the quality of the electron identification.

In order to increase the efficiency of the selection, cases where the candidate was either not isolated or not identified as a lepton were also treated. Kinematic requirements in this case were tighter, rejecting events if the angle between the direction of the missing momentum and the beam axis was $< 18°$ (30° for identified electrons) or if $\sqrt{s'}$, the effective centre-of-mass energy of the $q\bar{q}$ system if the event is interpreted as coming from the reaction $e^+e^- \to q\bar{q}\gamma$ [13], was $> E_{cms} - 15$ GeV.

Four-fermion backgrounds ($q\bar{q}\ell\ell$) were suppressed by applying an additional cut to events in which a second lepton of the same flavour and with charge opposite to that of the candidate was found. The event was rejected if the second lepton had momentum above 5 GeV/c and isolation angle with respect to all other particles except the candidate lepton above 15°.

In the selection of $jj\tau\nu$ events with the τ decaying hadronically, only events with at least 3 jets (found using the LUCLUS [14] algorithm with $d_{join} = 3$ GeV/c) were accepted, and the missing energy and the transverse energy were both required to exceed 40 GeV.

After selection of the lepton, it was required that the mass of the remaining particles, forced into 2 jets using LUCLUS, exceed 30 GeV/c^2, and that each hadronic jet have multiplicity of 4 or greater, at least one particle being charged. A 5-constraint kinematic fit was performed, imposing energy and momentum conservation and equal masses on the leptonic and hadronic W candidates. Tau candidates decaying hadronically were accepted if the mass of the hadronic system in the fit was above 65 GeV/c^2.

Application of these procedures to the 172 GeV data produced samples of 17 $jj\mu\nu$ events, 14 $jje\nu$ events and 9 $jj\tau\nu$ events, with estimated efficiencies of 90.3%, 74.6% and 36.8% in the three channels, respectively, and with an estimated background contamination of 0.356 ± 0.039 pb.

$jjjj$:
The criteria used to define the sample of events in this topology at 161 GeV have been given in [7]. In this procedure, the event was forced to a four-jet configuration, and the dominant background, which arises from the $q\bar{q}\gamma$ final state, was suppressed by requiring a variable D, $(= \frac{E_{min}}{E_{max}}\theta_{min}/(E_{max} - E_{min})$, where E_{min} and E_{max} are the energies of the jets with minimum and maximum energy and θ_{min} is the minimum interjet angle), to satisfy $D > 0.013$.

At 172 GeV, the requirement on D was replaced by two conditions: first, that the product of the three eigenvalues of the momentum tensor, given by LUCLUS, should exceed 0.025/27; and second, that at least one of the three kinematic fits which could be made to the event, imposing equality of two di-jet masses, should have $\chi^2 < 50$.

The selected $jjjj$ samples consisted of 15 events at 161 GeV and 52 events at 172 GeV, with estimated background contamination of 0.55 pb and 1.52 pb, respectively. The efficiencies for reconstructing events in the kinematically accepted region were found to be independent of TGC value to within the accuracy of the simulated statistics and equal to $\sim 70\%$ at both energies.

$\ell\nu\ell\nu$:

The criteria used to define the sample of events in this topology at 161 GeV have been given in [7]. In this procedure, low multiplicity events which satisfied a 2-jet description were accepted, thus allowing τ leptons as well as μ and e to be selected. Requirements on the minimum polar angle of the jets and on the direction of the missing momentum, set at $20^\circ < \theta_{jet} < 160^\circ$ and $|\cos\theta_{miss}| < 0.94$ at 161 GeV, were relaxed to $10^\circ < \theta_{jet} < 170^\circ$ and $|\cos\theta_{miss}| < 0.984$ at 172 GeV.

Samples of 2 events at 161 GeV and 7 events at 172 GeV were selected, with estimated efficiencies of $\sim$ 95%, $\sim$ 80% and $\sim$ 63% for selecting each μ, e and τ, respectively. Background contamination of 0.06 pb and 0.19 pb was estimated at the two energies, respectively.

jjX:
Events in this channel were required to have at least 6 good charged particles, and to produce at least 2 jets on application of the LUCLUS algorithm with $d_{join} = 5.5$ GeV/c. They were rejected if there was an energy deposition cluster of greater than 15 GeV in the electromagnetic calorimeter which was not associated with a charged particle. Accepted events were then forced into a 2-jet configuration, and the following energy-dependent selections applied:

At 161 GeV, the energy of each jet was required to exceed 20 GeV, and the polar angle to lie between 25°and 155°. The reconstructed invariant mass of the two jets was required to lie between 45 and 200 GeV/c^2. The missing momentum vector was required to satisfy $|\cos\theta_{miss}| < 0.9$, and the acollinearity and acoplanarity angles of the jets to satisfy $\theta_{acol} < 165^\circ$ and $\theta_{acop} < 169^\circ$, respectively.

At 172 GeV, these conditions were modified to: $E_{jet} > 10$ GeV, $15^\circ < \theta_{jet} < 165^\circ$, $m_{jj} > 50$ GeV/c^2, $E_{jj} < 100$ GeV, $|\cos\theta_{miss}| < 0.9$, $|\cos\theta_{acol}| < 0.98$ and $|\cos\theta_{acop}| < 0.98$, respectively.

Application of these procedures led to selection of 6 events at 161 GeV and 8 events at 172 GeV, with estimated efficiencies of 83% and 88% and backgrounds of 0.55 pb and 0.62 pb at the two energies, respectively. The principal background component is from the $q\bar{q}\gamma$ final state.

ℓX:
Only 161 GeV data were used in this channel because its relative contribution to the total four-fermion cross section at 172 GeV is much smaller. Candidate events were required to have only one track, clearly identified as a muon or electron. To reject cosmic ray background the normal track selections were tightened, requiring that the track pass within 1 cm of the interaction point in the xy plane (perpendicular to the beam) and within 4 cm in z. Lepton candidates were then required to have $p > 30$ GeV/c and $p_t > 25$ GeV/c. The leptonic selection efficienciea are as given above for the $\ell\nu\ell\nu$ final state.

One event was selected from the 161 GeV data, with negligible background.

While the final states considered above are topologically distinct, they are all represented by the generic e^+e^- interaction producing four final state fermions, $e^+e^- \to f_1\bar{f}_2 f_3\bar{f}_4$. In particular, the first three topologies ($jj\ell\nu$, jjX and ℓX) contain events in two different kinematic regions of the same four-fermion final state, $q_1\bar{q}_2\ell\nu$. In the $jj\ell\nu$ topology, the dominant amplitudes arising from diagrams with a triple vector boson coupling are

those contributing to WW production via s-channel γ and Z exchange; in the jjX and ℓXtopologies, the dominant amplitude involving a trilinear gauge coupling is that arising from radiation of a virtual photon from the incident electron or positron, leading to single W production, $e^+e^- \to We\nu$, with the final state electron lost in the beam pipe.

In the production of simulated events, we used the four-fermion generators EXCALIBUR [15] and GRC4F [16]. These generators were interfaced to the JETSET hadronization program [14], and to the full DELPHI simulation program DELSIM [12]. Samples of events were generated with both Standard Model and non-Standard Model values of TGC parameters, and were used both to determine the efficiency of the selection criteria in the topologies studied, and to check the accuracy of the analysis procedures in deriving the value of TGC parameters used in the generation of events. In addition, in the analysis of the $jj\ell\nu$ final state, a fast simulation of the DELPHI detector was used. Cross-checks were made to ensure that the fast and full simulations agreed in the distributions of the kinematic variables used in the analysis. The study of the backgrounds due to $q\bar{q}\gamma$ and ZZ production was made using fully simulated events generated with PYTHIA [17].

2.2 Selection of events for the study of $ZV\gamma$ couplings

The study of $ZV\gamma$ couplings involved a search for events containing only a single photon of high energy, emitted at large angle to the beam direction.

Such events were selected by requiring the presence of a "good quality shower" (defined in [12]) of energy $E_\gamma > 25$ GeV in the angular region $45° < \theta < 135°$, covered by the High density Projection Chamber (the barrel electromagnetic calorimeter). Events with a signal in the forward electromagnetic calorimeter were rejected, and a second shower in the barrel electromagnetic calorimeter was accepted only if it was within 20° of the first one. Events were also rejected if any charged particles were detected in the Time Projection Chamber, the main tracking device of DELPHI, or in the forward tracking chambers. The presence of charged particles not pointing to the interaction point also caused events to be rejected; this suppressed background from beam gas and cosmic events. In order to reject the background from radiative Bhabha and Compton events, no energy deposit was allowed in the Small Angle Tile Calorimeter (the luminosity monitor situated in the very forward direction). A further rejection of cosmic events was achieved by imposing a constraint on the γ direction: the line of flight and the shower direction measured in the calorimeter were required to coincide within 15°.

Application of these criteria produced samples of 8 events at 161 GeV and 7 at 172 GeV.

In order to estimate the cross-section for the single photon production process, the trigger and identification efficiencies must be known. The former was measured using radiative events ($\mu^+\mu^-\gamma$ and $e^+e^-\gamma$) and Compton events. The efficiency was shown to be dependent on the photon energy in the angular region under consideration, ranging from $\sim 65\%$ at $E_\gamma = 25$ GeV to $\sim 90\%$ for $E_\gamma > 40$ GeV. The identification efficiency was estimated using samples of 2500 fully simulated events at each energy, produced with the generator NUNUGPV [18]. It was found to to be practically constant for photon energies $E_\gamma > 25$ GeV and equal to 78%.

Various possible sources of background to the single photon production process were considered. The QED process $e^+e^- \to \gamma e^+e^-$ has a very high cross-section for low E_γ and when the two electrons escape undetected along the beam pipe, but it decreases rapidly

when E_γ and θ_γ increase, and contributes negligibly to the kinematic region selected. Other backgrounds, such as those from beam gas interactions, $\gamma\gamma$ collisions, $e^+e^- \to \gamma\gamma$, cosmic and Compton events were also found to be completely negligible.

3 Results on WWV couplings

It has been shown in previous studies [1] that the $jj\ell\nu$ topology provides the greatest precision in determination of WWV couplings. Here, we first give results from a detailed study of this final state using both total and differential cross-section information, then add the information obtained from the total cross-section of the $jjjj$ and $\ell\nu\ell\nu$ final states, and finally incorporate information from the "single W" topologies jjX and ℓX.

3.1 Results from $jj\ell\nu$ events

Two basic approaches have been used in the analysis of data from the $jj\ell\nu$ channel. In the first of these, based on an extension [19] of the method of Optimal Observables [20] described in [1], we use two variables which retain the full information of the 7-dimensional phase space describing the four-particle final state; in the second approach, distributions of well-measured variables, namely the W production angle, θ_W, and the polar angle of the lepton in the laboratory frame, θ_l, are analyzed. Our final results, reported in section 3.4, use TGC parameter values determined by the first of these methods for 172 GeV data and by the second method for 161 GeV data.

The analysis using the method of Optimal Observables exploits the fact that the differential cross-section, $d\sigma/d\vec{V}$, where $\vec{V}$ represents the phase space variables, is quadratic in TGC parameters: $d\sigma(\vec{V},\vec{\alpha})/d\vec{V} = c_0(\vec{V}) + \sum_i \alpha_i c_1^i(\vec{V}) + \sum_{ij} \alpha_i\alpha_j c_2^{ij}(\vec{V})$, where the sums are over the set $\vec{\alpha} \equiv \alpha_1 ... \alpha_N$ of parameters under consideration. In [19] it is shown that, in the case of the determination of a single parameter α, the distribution in the 2-variable space of $c_1(\vec{V})/c_0(\vec{V})$ and $c_2(\vec{V})/c_0(\vec{V})$ retains the whole information carried by the full distribution $d\sigma/d\vec{V}$ and hence allows determination of α with maximum precision. Furthermore, it is argued that little loss of precision is expected if the phase space variables $\vec{\Omega}$ available after reconstruction of events from experimental data are used in place of the true variables $\vec{V}$.

Data at 172 GeV were analyzed by performing a binned extended maximum likelihood fit to the two-dimensional distribution of $c_1(\vec{\Omega})/c_0(\vec{\Omega})$ and $c_2(\vec{\Omega})/c_0(\vec{\Omega})$ for each TGC parameter. The expected number of events in each bin was computed using the ERATO four-fermion generator [21] applied to samples of fully simulated events generated at a few values of the TGC parameters. A reweighting technique [22] was used to estimate the cross-section as a function of each parameter fitted. The results are shown in the first column of table 1. Figure 3.1 shows the distribution of the data in the $\left(c_1(\vec{\Omega})/c_0(\vec{\Omega}), c_2(\vec{\Omega})/c_0(\vec{\Omega})\right)$ plane, together with its projections onto the two axes and the expected distributions for the fitted value of one TGC parameter, $\alpha_{W\phi}$. The validity of the technique was verified by applying it to a large number of samples of fully simulated events corresponding to the same integrated luminosity as the data, generated both with Standard Model and non-Standard Model values of the couplings. The mean values of the precisions in the TGC parameters obtained from these samples were found to be compatible with those from the data, and the pull distributions had means and variances

compatible with 0 and 1 respectively.

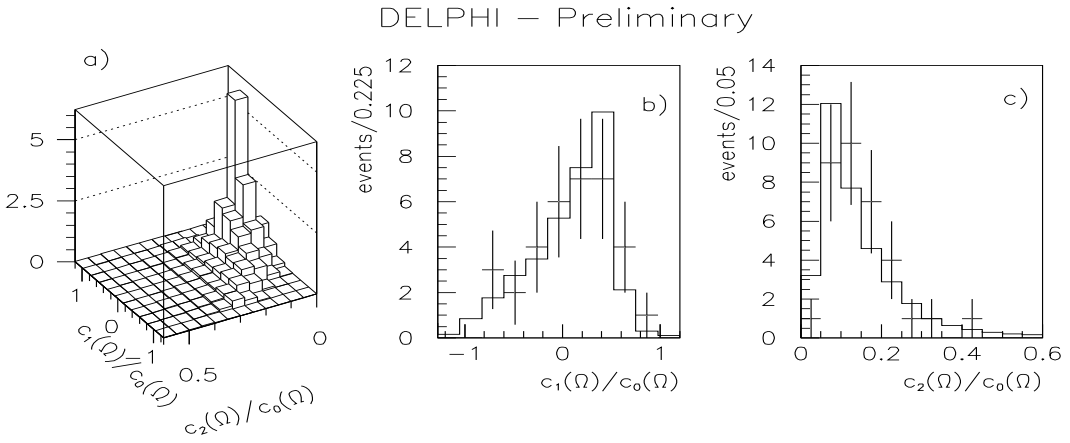

Figure 1: a) Distribution of $c_1(\vec{\Omega})/c_0(\vec{\Omega})$ versus $c_2(\vec{\Omega})/c_0(\vec{\Omega})$ for $\alpha_{W\phi}$ for 172 GeV data in the $jj\ell\nu$ topology. b) Projection onto the $c_1(\vec{\Omega})/c_0(\vec{\Omega})$ axis. c) Projection onto the $c_2(\vec{\Omega})/c_0(\vec{\Omega})$ axis. The points in b) and c) represent the data, and the histograms the expectation for the fitted value of $\alpha_{W\phi}$.

E_{cms}		Topologies used		
		$jj\ell\nu + jjjj + \ell\nu\ell\nu + jjX + \ell X$		
161 GeV	$\alpha_{W\phi}$	$-0.15^{+0.72}_{-0.68}$		
	α_W	$-0.34^{+1.24}_{-1.09}$		
	$\alpha_{B\phi}$	$0.23^{+1.22}_{-2.21}$		
172 GeV		$jj\ell\nu$	$jj\ell\nu + jjjj + \ell\nu\ell\nu$	$jj\ell\nu + jjjj + \ell\nu\ell\nu + jjX$
	$\alpha_{W\phi}$	$0.38^{+0.32}_{-0.32}$	$0.34^{+0.26}_{-0.29}$	$0.30^{+0.27}_{-0.28}$
	α_W	$0.28^{+0.57}_{-0.57}$	$0.25^{+0.50}_{-0.53}$	$0.22^{+0.48}_{-0.50}$
	$\alpha_{B\phi}$	$1.45^{+1.12}_{-1.47}$	$1.27^{+1.14}_{-1.36}$	$0.44^{+0.91}_{-1.03}$

Table 1: Results obtained from fits to TGC parameters at 161 and 172 GeV. For 172 GeV data, values are shown using information from the semileptonic topology $jj\ell\nu$ on its own, then with the addition of data from the from the $jjjj$ and $\ell\nu\ell\nu$ topologies, and then with addition of data from the single W topologies, jjX and ℓX.

Various systematic effects were considered, and the estimated errors incurred in the fitted TGC parameters at 172 GeV are summarized in table 2. The table contains contributions arising from the current precision of ± 100 MeV/c^2 in the value of the W mass [23], from the uncertainty in the LEP beam energy [24] and experimental luminosity, from the theoretical uncertainty in the cross-section evaluation (taken to be 2% [1]), from the granularity of the binning used, and from the errors in the estimated signal and background

cross-sections due to limited simulated statistics and from uncertainties in the selection procedure.

	$\alpha_{W\phi}$	α_W	$\alpha_{B\phi}$
Common systematics, 172 GeV:			
W mass	0.02	0.03	0.08
E_{cm}	0.02	0.02	0.04
Cross section	0.03	0.04	0.16
Luminosity	0.01	0.01	0.05
Topology $jj\ell\nu$, 172 GeV:			
Binning granularity	0.02	0.03	0.04
Signal estimation	0.02	0.03	0.12
Background estimation	0.01	0.02	0.06
Topologies $jjjj + \ell\nu\ell\nu$, 172 GeV:			
Signal estimation	0.04	0.05	0.06
Background estimation	0.03	0.03	0.04
Topologies $jjX + \ell X$, 172 GeV:			
Signal estimation	0.03	0.10	0.04
Background estimation	0.09	0.21	0.13
Combined systematics, 161 GeV:			
	0.07	0.10	0.15

Table 2: Estimated systematic errors in the determination of TGC parameters. Details of the common and topology-dependent contributions are shown for 172 GeV data; the total of all contributions is summarized for 161 GeV data. The entries for the $jj\ell\nu$ topology at 172 GeV refer to the analysis of the variables $c_1(\vec{\Omega})/c_0(\vec{\Omega})$ and $c_2(\vec{\Omega})/c_0(\vec{\Omega})$ described in the text.

In the second approach to the analysis of the $jj\ell\nu$ channel, several calculations were performed, studying both the joint distribution $(\cos\theta_W, \cos\theta_l)$ and the distribution of $\cos\theta_W$ on its own. These represent the best measured variables, with little bias involved in their direct estimation from the sum of the two measured hadronic jet vectors and the direction of the observed lepton, respectively. Both binned and unbinned maximum likelihood techniques were used, and calculations with three different four-fermion generators [16, 21, 25] were made. All gave compatible results. The results from an analysis of the 172 GeV data in which the binned distribution in the $(\cos\theta_W, \cos\theta_l)$ plane was compared with that computed using ERATO and a fast simulation of the detector response, are as follows:

$$\alpha_{W\phi} \;=\; 0.61\,^{+0.42}_{-0.49}(stat.)\,^{+0.11}_{-0.10}(syst.)\,,$$

$$\alpha_W = 0.91\,^{+0.59}_{-0.74}(stat.)\,^{+0.18}_{-0.19}(syst.)\,,$$
$$\alpha_{B\phi} = 1.74\,^{+1.20}_{-2.67}(stat.)\,^{+0.40}_{-0.40}(syst.)\,.$$

These results are in agreement with those from the Optimal Observable analysis, though, as expected, with rather lower precision. Figure 2 shows the distribution of the data in $(\cos\theta_W, \cos\theta_l)$ and its projections, with the expected distributions for the fitted value of $\alpha_{W\phi}$.

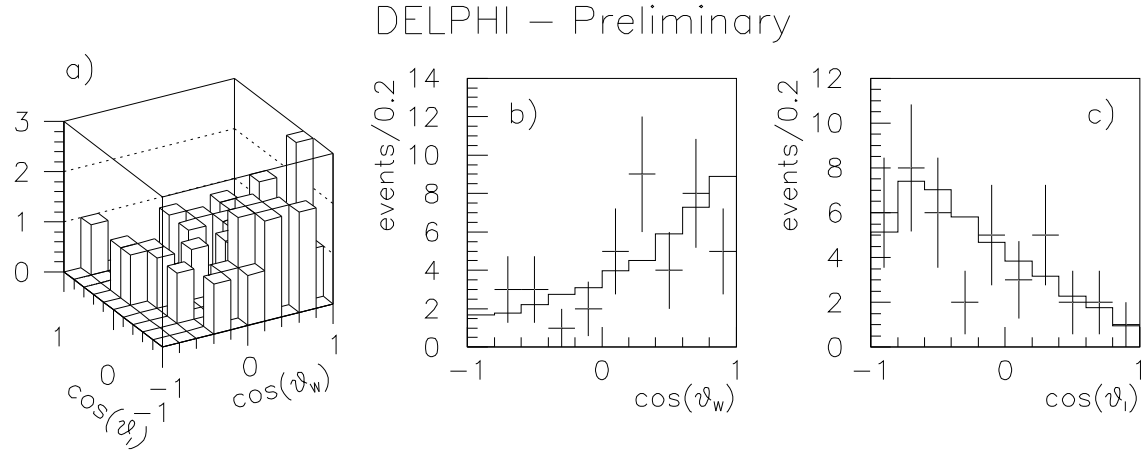

Figure 2: a) Distribution of $\cos\theta_l$ versus $\cos\theta_W$ for 172 GeV data in the $jj\ell\nu$ topology. b) Projection onto the $\cos\theta_W$ axis. c) Projection onto the $\cos\theta_l$ axis. The points in b) and c) represent the data, and the histograms the expectation for the fitted value of $\alpha_{W\phi}$.

The analysis of the 161 GeV data in the $jj\ell\nu$ channel was performed using only this analysis procedure, and the results, which have a much smaller statistical weight than those at 172 GeV, are combined with those from the channels considered below and given in table 1.

3.2 Inclusion of results from the $jjjj$ and $\ell\nu\ell\nu$ final states

Information from channels populated primarily by the fully hadronic and fully leptonic states from WW decays was added to that from the semileptonic topologies by comparing the observed total numbers of events observed with those expected as a function of TGC parameters. The GRC4F generator was used for the calculation, and fully simulated samples of events generated with EXCALIBUR at TGC values of -2, 0 and +2 were used to estimate the detector response. The values obtained by adding this information to that from the $jj\ell\nu$ topology are shown for 172 GeV data in the second column of results in table 1. Some increase in precision is evident. The systematic errors due to uncertainties in the estimation of signal and background cross-sections in these topologies are shown in table 2.

3.3 Inclusion of results from the jjX and ℓX final states

Information from the topologies to which the single W production process, $e^+e^- \to We\nu$, contributes significantly was added to that used in the WW channels considered above.

In the jjX topology, the observed number of events as a function of the W production angle (estimated from the sum of the two reconstructed jet directions) was compared with the number expected as a function of TGC parameters; in the ℓX topology, only the total cross-section information at 161 GeV was used.

Since the dominant mechanism for $We\nu$ production is via t-channel photon exchange, information from this region of the four-fermion phase space can, in principle, be used to measure the $WW\gamma$ couplings independently of WWZ couplings. However, the present statistics make this impracticable, and we choose instead to add this information to that from the WW topologies. The results are shown in the third column of results in table 1. Most of the parameters are hardly changed by addition of this data, but some improvement is seen in the precision in $\alpha_{B\phi}$; this has been confirmed by generator level studies, which indicate that the cross-section in the single W region is rather sensitive to this parameter. The systematic errors due to uncertainties in the estimation of signal and background cross-sections in these topologies are shown in table 2.

3.4 Combined results

Combining the results at 161 and 172 GeV given in table 1, we obtain final results for the TGC parameters:

$$\begin{aligned} \alpha_{W\phi} &= 0.24\,^{+0.26}_{-0.27}(stat.) \pm 0.06(syst.), \\ \alpha_{W} &= 0.14\,^{+0.46}_{-0.46}(stat.) \pm 0.09(syst.), \\ \alpha_{B\phi} &= 0.40\,^{+0.70}_{-0.91}(stat.) \pm 0.24(syst.)\,. \end{aligned}$$

A systematic error was assigned to each parameter by combining the contributions from the different topologies in table 2 according to their statistical weights, and adding the first four contributions in the table, considered as common to all topologies, in quadrature.

The parameter values shown are all consistent with zero, and hence with the expectations of the Standard Model.

4 Results on $ZV\gamma$ couplings

Using the sample of 15 events with $E_\gamma > 25$ GeV and $45° < \theta_\gamma < 135°$ selected from the combined data at 161 and 172 GeV as described in section 2.2, a cross-section

$$\sigma(e^+e^- \to \gamma \ + \ invisible\ particles) = 1.2 \pm 0.3(stat.) \pm 0.2(syst.)\ \text{pb}\,,$$

corrected for the experimental efficiencies in this region, was estimated. The systematic error comes mainly from the calorimeter energy scale and from the errors on the detection and trigger efficiencies.

The cross-section given above corresponds to a limit

$$\sigma(e^+e^- \to \gamma \ + \ invisible\ particles) < 1.9\ \text{pb}$$

at 95% C.L., including the effect of systematic errors. This limit is shown in figure 3 together with the predicted cross-section [26] as a function of the $ZV\gamma$ coupling parameters

h_{30}^{γ} and h_{30}^{Z}, defined in section 1. Limits at 95% C.L. of

$$|h_{30}^{\gamma}| < 0.5 \qquad \text{and} \qquad |h_{30}^{Z}| < 0.9$$

are derived at a scale $\Lambda = 500$ GeV. Figure 4 shows the region accepted at 95% C.L. in the $(h_{30}^{\gamma}, h_{30}^{Z})$ plane when both these parameters vary, using an energy scale of $\Lambda = 1000$ GeV and $n = 3$ in the form factor representation of h_3^V. For current values of $\sqrt{s}$, the data shows little sensitivity to the other CP-conserving vertex factors, h_4^V. If the analysis is extended to measure the CP-violating parameters h_{10}^{γ} and h_{10}^{Z}, the same limits are obtained as for h_{30}^{V}.

The results obtained for h_3^V show a considerable improvement over those reported previously from LEP data [10, 11], and are very close to the limits set by the Tevatron experiments [9].

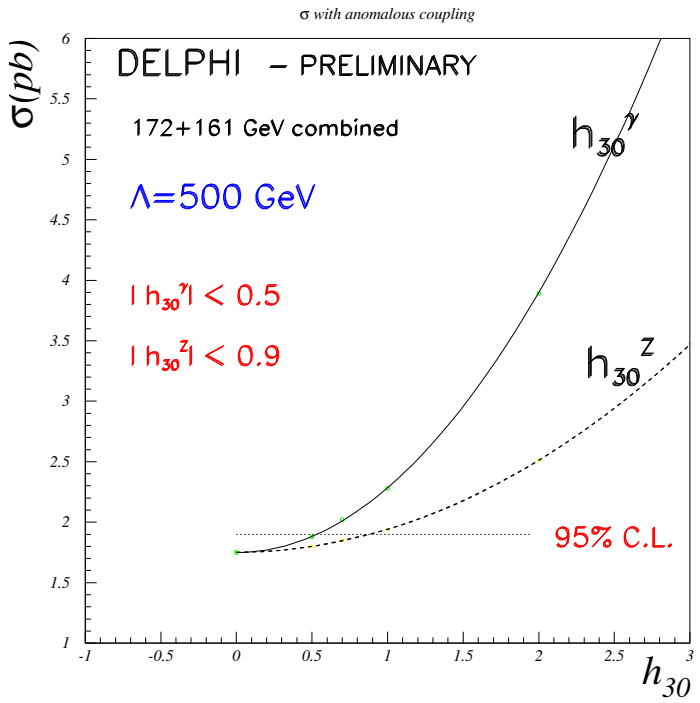

Figure 3: Upper limits at 95% C.L. on the $Z\gamma\gamma$ and $ZZ\gamma$ couplings from DELPHI single photon data at 161 and 172 GeV.

5 Conclusions

From integrated luminosities of 10.0 _and 9.98 _at centre-of-mass energies of 161 and 172 GeV, respectively, we have derived results summarized in section 3.4 for the WWV couplings $\alpha_{W\phi}$, α_W and $\alpha_{B\phi}$ using data from topologies populated both by WW production, $e^+e^- \rightarrow W^+W^-$, and by single W production, $e^+e^- \rightarrow We\nu$. We have also derived limits on the $ZV\gamma$ couplings $h_3^{\gamma,Z}$ using data from single photon production, with results given in section 4. We see no evidence in any of these results for deviations from Standard Model predictions.

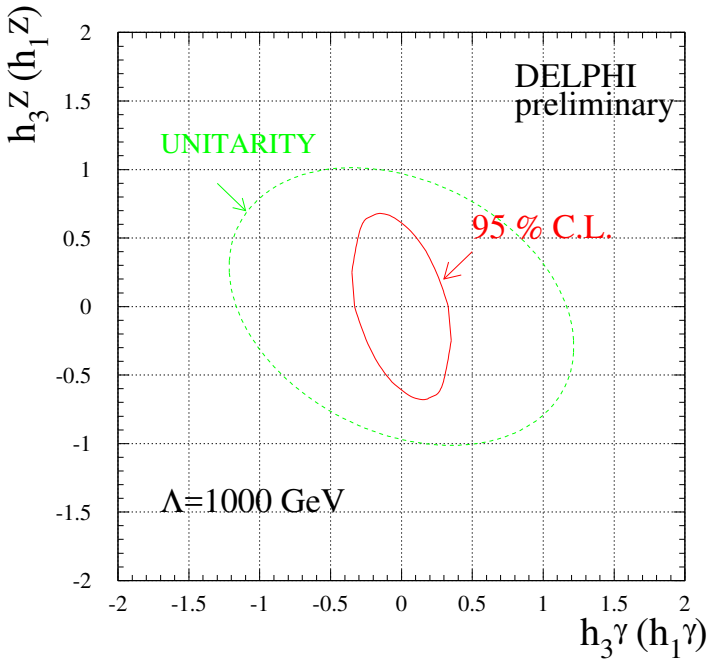

Figure 4: 95% C.L. contour for the $Z\gamma\gamma$ and $ZZ\gamma$ couplings h_{30}^{γ} and h_{30}^{Z} from DELPHI single photon data at 161 and 172 GeV. The limits are derived using an energy scale parameter $\Lambda = 1000$ GeV.

References

[1] G. Gounaris, J.-L. Kneur and D. Zeppenfeld, in *Physics at LEP2*, eds. G. Altarelli, T. Sjöstrand and F. Zwirner, CERN 96-01 Vol.1, 525 (1996).

[2] U. Baur and E. L. Berger, Phys. Rev. **D47** (1993) 4889.

[3] H. Aihara *et al.*, FERMILAB-Pub-95/031, MAD/PH/871, UB-HET-95-01, UdeM-GPP-TH-95-14, hep-ph/9503425 (1995).

[4] T. Yasuda, *Tevatron Results on Gauge Boson Couplings*, FERMILAB-Conf-97/206-E, to appear in the proceedings of the Hadron Collider Conference XII, Stony Brook, hep-ex/9706015 (1997).

[5] CDF Collaboration: F. Abe *et al.*, Phys. Rev. Lett. **74** (1995) 1936;
CDF Collaboration: F. Abe *et al.*, Phys. Rev. Lett. **78** (1997) 4536;
D0 Collaboration: S. Abachi *et al.*, Phys. Rev. Lett. **78** (1997) 3634.

[6] D0 Collaboration: S. Abachi *et al.*, Fermilab-Pub-97/088-E, hep-ex/9704004 (1997).

[7] DELPHI Collaboration, P. Abreu *et al.*, Phys. Lett. **B397** (1997) 158.

[8] DELPHI Collaboration, T. Bowcock *et al*, DELPHI 97-27 PHYS 675 (1997);
OPAL Collaboration, K. Ackerstaff *et al*, Phys. Lett. **B397** (1997) 147;
L3 Collaboration, M. Acciarri *et al*, CERN-PPE/97-14 (1997);
L3 Collaboration, M. Acciarri *et al*, CERN-PPE/97-28 (1997).

[9] CDF Collaboration, F. Abe *et al.*, Phys. Rev. Lett. **74** (1995) 1941;
D0 Collaboration, S. Abachi *et al.*, Fermilab-Pub-97/047-E (1997).

[10] L3 Collaboration, M. Acciarri *et al.*, Phys. Lett. **B346** (1995) 190.

[11] DELPHI Collaboration, P. Abreu *et al.*, Phys. Lett. **B380** (1996) 471.

[12] DELPHI Collaboration, P. Abreu *et al.*, Nucl. Inst. Meth. **A378** (1996) 57.

[13] P. Abreu, D. Fassouliotis, A. Grefrath, R.P. Henriques and L. Vitale, *SPRIME, A Package for Estimating the Effective* $\sqrt{s'}$ *Centre of Mass Energy in* $q\bar{q}(\gamma)$ *Events*, DELPHI note 96-124 PHYS 632 (1996).

[14] T. Sjöstrand, *PYTHIA 5.7 / JETSET 7.4*, CERN-TH.7112/93 (1993).

[15] F.A. Berends, R. Kleiss and R. Pittau, *EXCALIBUR*, Physics at LEP2, eds. G. Altarelli, T. Sjöstrand and F. Zwirner, CERN 96-01 Vol 2, 23 (1996).

[16] J. Fujimoto *et al., GRC4F*, Physics at LEP2, eds. G. Altarelli, T. Sjöstrand and F. Zwirner, CERN 96-01 Vol 2, 23 (1996).

[17] T. Sjöstrand, *PYTHIA 5.719 / JETSET 7.4*, Physics at LEP2, eds. G. Altarelli, T. Sjöstrand and F. Zwirner, CERN 96-01 Vol 2, 41 (1996).

[18] G. Montagna *et al.*, Nucl.Phys. **B452** (1996) 161.

[19] G.K. Fanourakis, D. Fassouliotis and S. Tzamarias, *Modified Observables; a maximum likelihood equivalent technique including detector effects*, DELPHI note 97-91 PHYS 715 (1997).

[20] M. Diehl and O. Nachtmann, Z. Phys. **C62** (1994) 397;
C.G. Papadopoulos, Phys. Lett. **B386** (1996) 442;
M. Diehl and O. Nachtmann, HD-THEP-97-03, CPTH-S494-0197, hep-ph/9702208 (1997).

[21] C.G. Papadopoulos, Comp. Phys. Comm. **101** (1997) 183.

[22] G.K. Fanourakis, D. Fassouliotis and S. Tzamarias, *Reweighting Technique for Monte Carlo Integration*, DELPHI note 97-56 PHYS 706 (1997).

[23] M. Rijssenbeek, *W mass from the Tevatron*, FERMILAB CONF-96/365-E, Proceedings of the 28th International Conference on High Energy Physics, Warsaw, (1996).

[24] A. Gurtu, *W production and mass measurements at LEP II*, to appear in the proceedings of the XIth Les Rencontres de Physique de la Vallee d'Aoste, La Thuile (1997).

[25] G. Montagna, O. Nicrosini and F. Piccinini, *et al., WWGENPV*, Physics at LEP2, eds. G. Altarelli, T. Sjöstrand and F. Zwirner, CERN 96-01 Vol 2, 23 (1996).

[26] To study this process in the DELPHI detector, the generator *NUNUGPV*, based on [18], was used.